Experimental demonstration of virtual critical coupling to a single-mode microwave cavity

Théo Delage, Olivier Pascal, Jérôme Sokoloff, Valentin Mazieres

Experimental Demonstration of Virtual Critical Coupling to a Single-Mode Microwave Cavity

Théo Delage,[1] Olivier Pascal,[1] Jérôme Sokoloff,[1] and Valentin Mazières[2]
[1)] *LAPLACE, Université Fédérale de Toulouse, 31062 Toulouse Cedex 9, France*
[2)] *ISAE-SUPAERO, Université Fédérale de Toulouse, 31055 Toulouse, France*

(*theo.delage@laplace.univ-tlse.fr)

(Dated: 24 March 2023)

We present an experimental realisation of the virtual critical coupling in microwave, *i.e.* the virtual perfect absorption of an incident wave by a resonant cavity, through the transient time modulation of its amplitude. The design of a waveform matched to the ignition process of a plasma, characterised in a simplified way by two operating modes over time (plasma off/plasma on) motivates this first step in the practical realisation of virtual critical coupling in microwaves. We propose a time domain method for extracting the necessary parameters for the realisation of the virtual critical coupling, especially the complex frequency called zero of the S-matrix. To this end, we start from the experimental characterisation of a single-mode and single-access microwave cavity including metal protrusions for future plasma ignition. Then, the method relies on the analysis of the harmonic response of the overcoupled cavity during three time periods: the transient under excitation, the steady state under excitation, and the transient after the excitation cut-off. Finally, an experimental demonstration of the virtual critical coupling is performed.

I. INTRODUCTION

Plasma source motivation and context: Plasma, frequently defined as the fourth state of matter, is an ionised and macroscopically electrically neutral gas[1]. The ignition of a plasma can be achieved by using electromagnetic energy. This energy is brought in different ways through devices called plasma sources[2]. The particularity of such plasma sources is their operation, i.e. the supply of energy, in two configurations over time: plasma off (transient before ignition) and plasma on (steady-state after ignition). Generally, the ignition of the plasma can strongly modify the properties of the plasma source[3]. In the context of RF or microwave plasma sources, for instance the ignition of plasma into a microwave cavity, it can lead to a mismatch between the cavity and the energy generator, and in the worst case, to the extinction of the plasma. This mismatch affects the efficiency of the energy transfer between the generator and the cavity. As the powers involved can be significant, the reflection caused by the mismatch can be a problem for the components placed before the cavity receiving the plasma. Strategies to overcome the reflection problem are then to absorb and dissipate this reflection by adding isolators or circulators. More sophisticated matching techniques are based on careful dimensioning or geometrical adjustment of the structure, or the use of impedance matching systems[4]. All these techniques rely on adjusting the system, but not the excitation.

Recently, a new type of plasma source was developed. Inspired by works about time reversal of electromagnetic waves[5], it is based on the spatio-temporal control of microwaves by the shaping of the temporal waveform transmitted to a cavity. It allows the space-time steering of microwave plasmas[6,7]. However, the design of this method mainly considers the plasma-off configuration and does not lead to a matched cavity in the two operating modes. On the other hand, the idea of playing on the shape of the excitation of the plasma source could be extended to match the generator signal during the ignition process, considering the cavity's properties would evolve in time[8]. Moreover, the ignition phase is transitory, which leads us to consider transient shapes of excitations.

Towards a matched transient excitation: In this way, also considering resonant systems such as cavities, the unusual phenomena of wave scattering, characterised by spectral singularities, have received significant attention in recent years[9]. We can for example mention the theory of reflectionless scattering modes, a general theory for impedance matching of waves in complex scattering structures and geometries (multichannel, overlapping modes, etc)[10]. Coherent perfect absorption can then be seen as a special case of this theory, for which impedance matching is possible by adding dissipative losses to the scattering system, leading to purely irreversible loss mechanisms[11]. However, these concepts refer to stationary phenomena, and some of them, such as coherent perfect absorption for which energy is dissipated, do not lead to a significant electromagnetic energy rise of the resonator (that is useful in order to ignite a plasma).

Lately, the idea of virtual absorption[12] has provided a new perspective on the transfer of energy from a generator to a resonant structure. This concept highlights transient phenomena during the coupling of energy to the cavity. It allows to observe the excitation of a resonator without reflection or transmission, with most of the incident energy stored inside for the limited time of the excitation. It is based on the temporal modulation of the resonant structure itself[13,14], or on the temporal modulation of the generator[12,15–18]. The latter option has been studied experimentally for elastodynamic waves[19] and water waves[20]. It has also been theoretically and numerically applied to the excitation signal of a single-mode cavity coupled to a single access. Referring to the well-known critical coupling[21], this led to the formulation of the concept of virtual critical coupling[22] (note that a generalization to multi-access resonator is possible). In this case, the modulation of the oscillating incident signal consists in shaping an exponential growth of its amplitude, characterised by a precise com-

plex frequency. These conditions make it possible to balance the exponential growth of the signal amplitude that leaks from the cavity during excitation by destructive interference. This leads to the transient excitation of the resonant structure without scattering. This compensation is achievable for a discrete number of complex frequencies, called zeros of the S-matrix. They are more generally part of what are called singularities of the S-matrix[9,23]. Note that we will use the term real frequency to refer to the usual frequency. This real frequency is actually the real part of the complex frequency. Its imaginary part reflects an exponential modulation of the signal amplitude.

On extracting S-matrix zeros for experiment: Although the singularities of the S-matrix have been described theoretically[9,23], many works are interested in how to extract them for practical scattering systems. The Harmonic Inversion technique[24,25] is widely documented and used in order to identify the resonances, i.e. the poles of the S-matrix, of a scattering system which may be multi-channel and multimodal with overlapping[26,27]. However, the search for the zeros of the S-matrix via this method is little mentioned[28], or even rejected because it seems less direct[29]. For the extraction of the S-matrix zeros, in the article about coherent virtual absorption of elastodynamic waves[19], the S-matrix of the experimental device has been formulated analytically as a function of frequency. However, the S-matrix of most scattering systems cannot be easily specified in this way. Recently, many efforts have been made to encounter the zeros of the S-matrix from experimental data. Most of them are in fact based on parametric analysis and optimisation of the absence of scattered waves for real frequencies, i.e. zeros placed on the real axis. The parametrisation can be done by frequency and attenuation sweeps, leading to the extraction of zeros at arbitrary real frequencies[30,31]. Other efforts have been made to fix the real frequency of the zero, via the use of metasurfaces[32–36]. However, these solutions imply modifying the resonator properties at each parametric variation (attenuation with localised loss modulation or configuration change of the metasurface). The generalization of these methods is difficult to consider in order to find complex zeros of a given resonator, which are sought to achieve virtual absorption. Moreover, the optimisation time might be problematic for the purpose of adapting the cavity (and not the generator signal) between plasma off and plasma on configurations. Optimisation and analytical description are also used to try to identify and observe the coalescence of several real zeros[37,38]. Finally, we must mention the very recent work that seems to offer a way to extract the zeros of the S-matrix from the experimental measurement of the latter[29,39]. So far, this frequency method works for multichannel resonators and isolated resonances. These different works show the complexity of the extraction of singularities of the S-matrix from real practical scattering systems and experimental measurements. Yet, the realisation of virtual critical coupling for a given cavity relies on the knowledge of the zeros of the S-matrix.

Organisation of the paper: The objective of the work presented in this paper is the experimental demonstration of virtual critical coupling for a microwave resonant cavity. In Sec. II, we present the single-mode and single-access cavity including metal protrusions on which our experimental demonstration is based. Sec. III recalls the theoretical bases associated with the excitation of the S-matrix zero of our cavity. To achieve our main objective, we propose in Sec. IV an alternative time domain method to extract the complex frequency associated with this zero. This time domain method is based on the measurement of the resonator S-matrix and, on the analysis of the harmonic response of the cavity, in line with the study of virtual critical coupling in the article mentioned above[22]. Finally, we show in Sec. V, the practical realisation of the excitation of a S-matrix zero of our cavity, in other words, to the authors' knowledge, a first experimental realisation of virtual critical coupling in the microwave domain.

II. PRESENTATION OF THE CAVITY

To study virtual critical coupling in practice, we choose a single-access, single-mode cavity that works in a frequency band suitable for the instrumentation available to us (see Sec. V). Recently in our laboratory, B. Fragge *et al.* were interested in the design of a plasma source at atmospheric pressure in a microwave cavity for the ignition of liquid fuels[40]. The microwave cavity for the realisation of a virtual critical coupling excitation is the one designed and characterised in the cited article. This versatile aluminium cavity (AU4G 2017A), forms a rectangular parallelepiped, and is coupled to a microwave generator through a copper coaxial probe partly surrounded by PTFE. One of the original features of this cavity is the possibility to place concentrators, i.e. metal rods facing each other, forming a gap in which the electric field is concentrated, which favours the ignition of plasma (see Fig. 1b). For the excitation of the TE_{012} resonant mode, these are located on a maximum electric field. This electric field is even more concentrated in the gap. This has allowed the ignition of non-equilibrium plasmas, in air and at atmospheric pressure, for an incident power of 200 W[40].

We propose to consider the cavity in the presence of cylindrical concentrators for this study, which sets the resonance of the desired mode around 2.41 GHz. Moreover, this configuration makes it difficult to express its S-parameters analytically. This makes us consider an alternative method for the extraction of S-matrix singularities of this cavity necessary for the realisation of virtual critical coupling (see Sec. IV). Fig. 1a illustrates the cavity through the 3D electromagnetic simulation software HFSS. It gives the reader an idea of the architecture of the structure and the electric field distribution for the TE_{012} resonant mode.

III. THEORETICAL BACKGROUND

The main objective of this paper is to excite the desired resonant mode of the cavity described in the previous section with transient suppression of reflection of the incident signal. The careful design of the excitation should thus lead to the full transfer of the incident energy to our cavity. This cavity

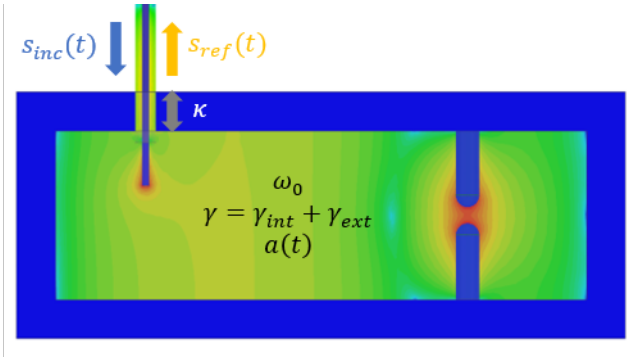

(a)

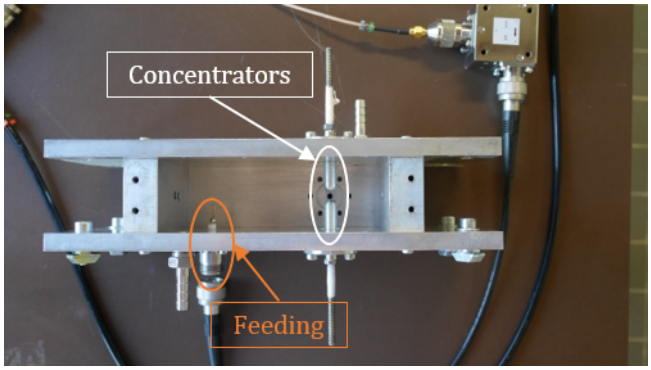

(b)

FIG. 1: (a) Electric field calculated by the HFSS solver for resonant cavity excitation around 2.41 GHz. This versatile cavity for plasma ignition at atmospheric pressure, widely described in[40], measures $136 \times 86 \times 43$ mm^3 here, and is excited through a 14 mm long coaxial feeding to allow overcoupling. Two 20 mm long cylindrical concentrators are positioned 30 mm from the right wall, at the location of an electric field peak. The physical parameters to be considered for the analytical study of the temporal dynamics are also illustrated. (b) Photograph of the cavity considered in this paper, with a side face removed. We can identify the concentrators, also called "initiators" in the article already mentioned[40].

is coupled to a single access, is single-mode in the real frequency band of interest (presence of a single resonance), and has intrinsic losses.

The temporal coupled mode theory (TCMT)[41,42] synthesises, through two equations, the energy exchanges between the scattering system's eigenmodes and the coupling of these modes to one or more incident signals. As detailed in the literature[9,14,22], it can be used to describe the scattering properties of our cavity over time. Thus, applied to our single-mode and single-access cavity, we write the dynamic equation of the resonance amplitude of the mode :

$$\frac{da(t)}{dt} = (j\omega_0 - \gamma_{int} - \gamma_{ext})\, a(t) + \kappa s_{inc}(t) \tag{1}$$

and the equation for the global reflected signal :

$$s_{ref}(t) = -s_{inc}(t) + \kappa a(t) \tag{2}$$

Fig. 1a illustrates the intrinsic characteristics of the cavity and those related to the coupling of a signal through its unique access. The cavity is characterised by a resonant normal mode at the angular real frequency ω_0 and a decay rate γ. The latter specifies the way in which the energy stored in the cavity is lost. A distinction is made between intrinsic losses by dissipation at the walls (γ_{int}) and external losses by the leakage of energy from the resonator to the coaxial feed (γ_{ext}). Each decay rate is associated with a quality factor according to the expression $Q = \omega_0/2\gamma$. We write $a(t)$ the resonance amplitude[41] of the mode, and $|a(t)|^2$ defines the energy stored over time. Finally, we provide energy via the incident signal $s_{inc}(t)$, and characterise the coupling of this signal to the cavity by the κ coefficient. The latter is directly related to the external decay rate by[42] $\kappa = \sqrt{2\gamma_{ext}}$. The reflected signal that may result from this coupling is denoted $s_{ref}(t)$. The squared modulus of these signals describes the incident and reflected powers respectively. With these details, we see that Eq. (2) describes the reflected signal as the superposition of two contributions. The first is linked to the direct reflection of the incident signal at the cavity access. The second is related to the energy leakage from the cavity to the coaxial cable.

From these two equations, we can establish the conditions for cancellation of the reflected signal in time. For a time convention in $e^{j\omega t}$ ($s_{inc}(t) \sim e^{j\omega t}$), and assuming the complex angular frequency plane with $\omega = \omega' + j\omega''$, we adopt from the literature the expression of the reflection coefficient $r = s_{ref}/s_{inc}$ as a function of the excitation complex angular frequency[22] :

$$r(\omega', \omega'') = \frac{(\gamma_{ext} - \gamma_{int} + \omega'') - j(\omega' - \omega_0)}{(\gamma_{ext} + \gamma_{int} - \omega'') + j(\omega' - \omega_0)} \tag{3}$$

We then see the existence of the singular complex angular frequency $\omega = \omega_0 + j(\gamma_{int} - \gamma_{ext})$ which allows the cancellation of the numerator of Eq. (3). It thus gives a condition on the incident signal to achieve cancellation of the reflected signal during the excitation. This complex angular frequency is one of the singularities of the reflection coefficient. Since our cavity has only one access, studying this reflection coefficient is in fact the same as being interested in the S-matrix of the resonator. This complex angular frequency is then generalizable as a singularity of the S-matrix, and is called zero of the S-matrix[9]. We can write it ω_{zero}. It satisfies the ingoing boundary condition[9,23]. Thus, an excitation signal of the form $s_{inc}(t) \sim e^{j\omega_0 t} e^{(\gamma_{ext} - \gamma_{int})t}$, should theoretically allow us to transfer energy to the cavity without reflection, and more generally without back-scattering, for the time of the excitation.

For $\gamma_{int} = \gamma_{ext}$, this complex angular frequency becomes pure real and we find the so-called critical coupling condition. In this case, a sinusoidal excitation (CW) fulfils the ingoing boundary condition. In order to obtain this equality, it is necessary, for example, to modify the length of the coaxial feed in the cavity (modification of γ_{ext}), or to add absorbers in the cavity (modification of γ_{int}). However, it has been shown that this excitation is not necessarily the most efficient in terms of energy stored in the resonant system compared to the amount of incident energy (excitation efficiency[22]). In fact, a large part of the latter is directly dissipated[22]. Also, during the transient

phase of the excitation, *i.e.* a thousand periods of the incident signal (about 450 ns) for our cavity with the adjusted size of the monopole, this coupling presents an important part of reflected energy. Nevertheless, this strategy is usually sought and implemented when one wishes to transfer energy to a resonant device[43].

The originality recently highlighted consists in understanding that even if the cavity is not matched in the classical sense of the term, *i.e.* with different intrinsic and external quality factors, it is possible via the temporal modulation of the excitation, to force the transient absorption of the excitation signal by the cavity[22]. Specifically, in the case where $\gamma_{int} < \gamma_{ext}$, for which the cavity is said to be overcoupled, the time modulation consists of generating an incident signal with an exponentially increasing amplitude over time. We then speak of virtual absorption[12,15–17,19], or in reference to the usual case mentioned above, of virtual critical coupling[22]. An excitation whose amplitude increases exponentially does not seem to be sustainable over long periods of time. However, it presents the advantage of not necessarily having to seek to modify the resonant system to limit the reflection. Also, virtual critical coupling seems to pave the way to the matching of the excitation signal to a cavity whose properties would evolve in time, for example during the ignition of a plasma[8]. Unlike the classical critical coupling, it allows an excitation efficiency close to unity[22].

Moreover, let us note that the complex angular frequency $\omega = \omega_0 + j(\gamma_{int} + \gamma_{ext})$ makes it possible to cancel the denominator of Eq. (3). We have here a new singularity of the S-matrix, called the pole, and satisfying the outgoing boundary condition[9,23]. In other words, the cut-off of the excitation, thus the absence of incident wave on our cavity, will lead to the release of the energy stored in the cavity during the excitation period. This takes place according to an exponential decay at this complex angular frequency.

Finally, in the case of a cavity with no intrinsic losses ($\gamma_{int} = 0$), time-reversal symmetry imposes that the poles and zeros of the S-matrix are conjugate. When the cavity has intrinsic losses, as in the case of our cavity, this symmetry is broken and the poles and zeros are no longer conjugate[9].

IV. TIME DOMAIN METHOD TO EXTRACT S-MATRIX SINGULARITIES OF THIS CAVITY FROM THE EXPERIMENTALLY MEASURED S-MATRIX

Now that we have recalled some theoretical bases, we wish to determine the pole and the zero of the S-matrix for the TE_{012} resonant mode of our cavity. The final objective is to excite the zero and realise virtual critical coupling. It requires the extraction of the intrinsic and external decay rates associated with our scattering system, consisting of the cavity and its coaxial feed, and for the resonant mode considered. In this section, we propose a time domain method for extracting these complex angular frequencies from the S-matrix of the cavity. This approach is based on several steps summarised in Table I which we will detail through the direct application to the cavity described previously.

TABLE I: Proposed time domain method for the extraction of the S-matrix singularities of our cavity for the purpose of exciting a S-matrix zero. $\mathscr{F}$ refers to Fourier transform.

Step	Description
A. Identification of ω_0	S_{11} overcoupled $\rightarrow$ Choice of ω_1 $\rightarrow s_{ref}(t) = \exp(j\omega_1 t) * s_{11}(t)$ $\rightarrow \mathscr{F}\left[s_{refcut-off}(t)\right]$ $\rightarrow \omega_0$
B. Identification of γ_{int} and γ_{ext}	$r(t) = s_{ref}(t)/\exp(j\omega_0 t)$ $\rightarrow t_{r=0}$ and r_∞ $\rightarrow \gamma_{int}$ and γ_{ext}
C. Verification of zero reflection	$\omega_{zero} = \omega_0 + j(\gamma_{int} - \gamma_{ext})$ $\omega_{pole} = \omega_0 + j(\gamma_{int} + \gamma_{ext})$ $\rightarrow$ Plot of $s_{ref}(t) = \exp(j\omega_{zero} t) * s_{11}(t)$

A. Identification of pole and zero real part ω_0

As seen in Table I, the identification of ω_0 is done through different operations. Recall that the theory expresses ω_0 as the real part of the pole and zero of the single-mode cavity. The first step consists in acquiring the spectrum of the S-matrix. Here, it involves measuring the modulus and phase of $S_{11}(\omega)$ in the frequency band of interest. Fig. 2 illustrates the spectrum of S_{11} that we measured with the Keysight E5071C Vector Network Analyser (VNA) over the 2.2 to 2.6 GHz band. The modulus indicates a cavity resonant mode around 2.41 GHz, with a minimum at -1.2 dB. This means a significant steady-state reflection level for CW excitation. We are clearly not in the presence of a critically coupled cavity, for which this modulus of the reflection coefficient would be much lower. The phase must then be observed to understand that we are in the presence of an overcoupling of the cavity. Indeed, for an undercoupling regime, it is the contribution of the direct reflection at the access that dominates. This contribution and the incident signal are 180° out of phase. Thus, the phase of S_{11} at resonance on the spectrum remains at $\pm\pi$. In contrast, for a case of overcoupling such as this one, it is the contribution of the leakage from the cavity to the coaxial cable that constitutes the major part of the global reflected signal. Then we see around the resonance a continuous evolution of the phase between $+\pi$ and $-\pi$. It is particularly the phase transition through 0 that is of interest for the excitation of the zero of the S-matrix.

Two intermediate steps are necessary to obtain the real part of the pole and the zero. We know that the pole associated with the excited mode corresponds to the complex angular frequency of the release signal observed in the absence of an incident wave (outgoing boundary condition[23]). This complex angular frequency is unique whatever the real or complex angular frequency of the initial mode excitation signal, considering a single-mode resonator (see supplementary materials, sec. I). To obtain the release signal associated with the mode, the first of these steps is to fill the cavity. For example, we choose a harmonic excitation $s_{inc}(t) = e^{j2\pi f_1 t}$ at the real frequency $f_1 = 2.4085$ GHz corresponding to the zero phase

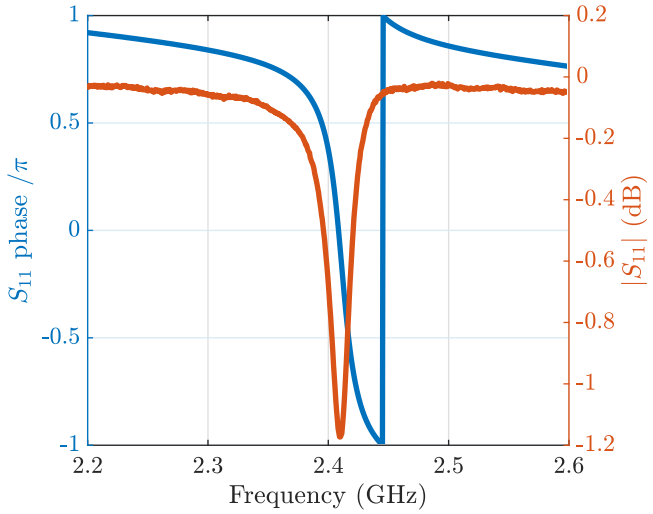

FIG. 2: Measured reflection coefficient S_{11} spectrum of the electromagnetic cavity.

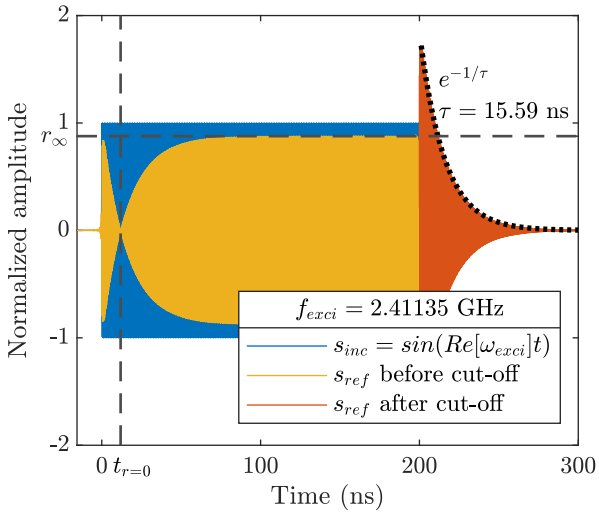

FIG. 3: Numerical construction of the temporal response of the cavity from a CW excitation at the real part of the frequency of the singularities at the studied resonance. In the legends, $\omega_{exci} = 2\pi f_{exci}$ refers to the frequency of the incident excitation signal.

of the measured S_{11}. The response $s_{ref_{num}}(t)$ of the cavity to this excitation, using the measured S_{11} as a transfer function, can be written $s_{ref_{num}}(t) = s_{inc}(t) * s_{11}(t)$ in the time domain, which gives in the frequency domain by application of the Fourier transform $\mathscr{F}$:

$$\mathscr{F}\left[s_{ref_{num}}(t)\right] = \mathscr{F}\left[s_{inc}(t)\right] \cdot S_{11}(f) \tag{4}$$

We numerically construct this signal in the time domain by inverse discrete Fourier transform. We obtain a response similar to the one plotted on Fig. 3 (not for f_1 in this figure, see supplementary materials sec. I for the one corresponding to the f_1 excitation). Note that for all such chronogram in the article, the yellow part corresponds to the reflected signal before excitation cut-off, *i.e.* the time interval during which the incident signal in blue is different from zero. The red one corresponds to the reflected signal after excitation cut-off (the incident signal is zero). For each of the figures, the reflected signal is calculated or measured at once, the colour differentiation (yellow and red) being only a visual distinction. Moreover, the chosen time interval does not allow the oscillations of the signals (with a period of about 0.4 ns) to be visually distinguished.

Then, to identify the real part of the pole, we carry out a spectral study of the signal scattered by the cavity after excitation cut-off (in red). The observed exponential decay, characterised by a time constant of 15.59 ns, is displayed in Fig. 4 as a Lorentzian in the frequency domain. This is centred on a real frequency, invariant to the way the cavity mode was excited (real or complex angular frequency - see supplementary materials sec. I). It is the real part of the pole of the S-matrix, and by identification thanks to the theory for our case, that of the zero. We note it $\omega_0 = 2\pi f_0$, with in our case $f_0 = 2.41135$ GHz. Let us add that the linewidth $\Delta\omega = 2\pi\Delta f$ of the Lorentzian is proportional to the imaginary part of the pole ($\Delta\omega = 2Im[\omega_{pole}]$), and inversely proportional to the time constant of the decay ($\tau = 1/Im[\omega_{pole}]$).

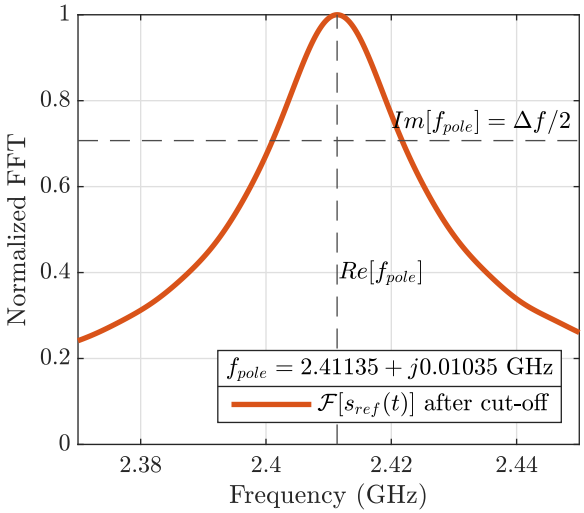

FIG. 4: Frequency spectrum of the scattered signal after the CW excitation cut-off (in red on Fig. 3). The centre frequency of the Lorentzian corresponds to the real part of the pole (and consequently the zero), $\omega_0 = 2\pi.Re[f_{pole}] = 2\pi f_0$. The imaginary part of the pole is estimated here from the Lorentzian linewidth Δf.

B. Identification of the decay rates γ_{int} and γ_{ext}

Now, let us consider the peculiar case of the harmonic excitation of the cavity at the real part of the pole and the zero, $s_{inc}(t) \sim e^{j\omega_0 t}$, without stored energy at $t = 0$. Eqs. (1) and (2) of the TCMT applied to our cavity allow us to formulate the temporal evolution of the reflection coefficient

$r(t) = s_{ref}(t)/s_{inc}(t)$ as a function of the decay rates:

$$r(t) = \frac{2\gamma_{ext}}{\gamma_{ext}+\gamma_{int}}\left(1 - e^{-(\gamma_{ext}+\gamma_{int})t}\right) - 1 \tag{5}$$

We can also build up the reflected signal during excitation associated with this special case, using the numerical method described earlier. Fig. 3 shows the result of this construction. The signals are normalised by the maximum amplitude of the incident signal. The envelope of the normalised reflected signal (in yellow) then represents the time evolution of the reflection coefficient. This evolution is expressed analytically by Eq. (5). We can observe a transient period characteristic of overcoupling[22]. Indeed, the reflection decreases until an instant of zero reflection, before increasing to reach the steady state. At the cut-off of the excitation, we find the exponentially decaying amplitude signal associated with the pole of this cavity resonance (in red). Note that this type of response to CW excitation, including during the transient phase, could be observed through the experimental set-up described in the next section, and can be used directly to fit the theory at the cost of more noise and uncertainty (see supplementary materials sec. II).

Then, from Eq. (5), we derive a system of two equations with two unknowns to calculate γ_{int} and γ_{ext}. A first equation comes from the knowledge of the instant $t_{r=0}$ for which the reflection coefficient cancels during the transient phase, $r(t) = 0$. The second equation is found by considering the reflection coefficient in the steady state, *i.e.* the measurement of r_∞ for $t \to \infty$ during the excitation. From these equations, we identify the intrinsic decay rate:

$$\gamma_{int} = \frac{1-r_\infty}{2t_{r=0}} \ln\left(\frac{1+r_\infty}{r_\infty}\right) \tag{6}$$

and the external decay rate :

$$\gamma_{ext} = \frac{1+r_\infty}{2t_{r=0}} \ln\left(\frac{1+r_\infty}{r_\infty}\right) \tag{7}$$

Finally, the knowledge of these decay rates leads us to find the imaginary part of the pole (which could already be calculated using the spectral analysis of the exponential decay of the cavity leakage signal at the excitation cut-off) $\omega''_{pole} = \gamma_{ext} + \gamma_{int}$, and to calculate the imaginary part of the zero $\omega''_{zero} = \gamma_{int} - \gamma_{ext}$, which we are mainly interested in. Table II summarises the quantities calculated through our extraction time domain method.

C. Verification of zero reflection with a plot

The last step is to verify the validity of the identified zero by a new numerical construction. As before, we calculate from the spectrum of S_{11} measured with the VNA, the signal reflected over time by the cavity for the ideal excitation of the zero of the S-matrix. This ideal incident signal, constructed numerically, is of the form $s_{inc}(t) = s_0 e^{j(\gamma_{ext}-\gamma_{int})t} e^{j\omega_0 t}$, with s_0 the amplitude of the incident signal at $t = 0$. The result is plotted in Fig. 5. We observe the absence of reflected signal during the excitation period (in yellow), confirming the possibility of exciting a zero of the S-matrix of our cavity. Finally, at the cut-off of the excitation, we observe, as in the case of the CW excitation, the decaying signal that leaks out of the cavity through the pole associated with the resonance under study. The observed exponential decay has the same time constant as in Fig. 3, also calculated in Table II.

In this section, we have shown a time domain method for extracting the pole and the zero of a single-channel, overcoupled, single-mode cavity over a fairly wide frequency band. This extraction has been carried out from the S-matrix via its spectral measurement with a VNA. This time domain method enables to verify that proper design of the incident signal should allow the virtual critical coupling to be achieved, even in the presence of intrinsic losses. It relies on the analysis of the temporal waveform of the reflected signal in order to

TABLE II: Characteristics of the cavity found by our extraction time domain method. Here, the sign of the imaginary parts of the pole and the zero is imposed by our convention in $e^{j\omega t}$. Injected into this, we find an exponentially decaying amplitude for the pole, growing for the zero[23].

ω_0	2π·(2.41135 GHz)
$t_{r=0}$	11.86 ns
r_∞	0.8773
$Q_{int} = \omega_0/(2\gamma_{int})$	1926
$Q_{ext} = \omega_0/(2\gamma_{ext})$	126
ω''_{pole}	2π·(0.01021 ·10^9) Np/s
ω''_{zero}	-2π·(0.00896 ·10^9) Np/s
τ	15.59 ns

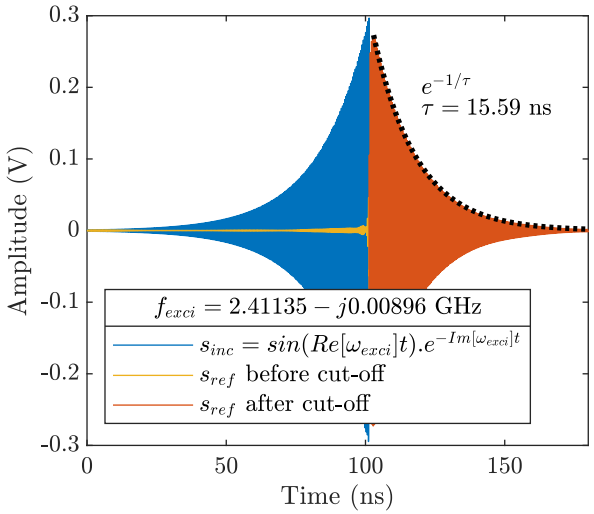

FIG. 5: Numerical construction of the temporal response of the cavity from the zero excitation. Here, the initial peak amplitude of the incident signal is set to 0.5 mV, and the duration of the excitation is set for a final peak amplitude of 0.3 V.

extract S-matrix singularities, with the theory hypothesis that the pole and zero real parts are similar (see Eq. (3)). Hence, it seems of particular interest for analysing time-varying cavities, such as cavities used for plasma ignition[3,8]. It is the practical way of shaping the incident signal that will interest us in the following part in order to really excite this zero.

V. EXPERIMENTAL GENERATION OF THE CAVITY S-MATRIX ZERO

A. Experimental set-up

Fig. 6 shows a schematic and a picture of the experimental set-up for the purpose of performing and characterising the zero excitation for mode TE_{012} of the cavity presented in the plasma context, around 2.41 GHz. For this purpose, our experimental work relies on Keysight's 33600A Arbitrary Waveform Generator (AWG), offering a bandwidth of 120 MHz. This generator is used to design the envelope of the incident signal. This envelope can be found in green in Fig. 7. A Tektronix TSG4104A RF signal generator is used to generate the carrier of the incident signal. With a resolution of 1 μHz in the 950 kHz - 4 GHz band, it will be able to generate the harmonic signal at the real part of the zero with the required accuracy. The final construction of the incident signal goes through a Polyphase QM2040A modulator, operating between 2 and 4 GHz. It receives the AWG envelope on the I channel, with the Q channel shorted, and performs the carrier modulation.

To characterise the validity of the zero excitation, we wish to measure the signals incident on and reflected by the cavity. We have therefore chosen to create two measurement channels, incident and reflected, by the presence of a power splitter, operating between 2 and 4.2 GHz. The information carried by the signal at the output of the modulator is therefore found on both channels, but attenuated by about 3 dB. The output of the power splitter to the incident channel is fed directly to the oscilloscope through coaxial cables. The signal output on the other channel of the power splitter should be directed to the cavity. A circulator operating between 2.4 and 2.6 GHz is placed just before the cavity to direct the reflected signal to the oscilloscope. It also isolates this measurement from a contribution from the incident signal. An isolator is placed between the power splitter and the circulator to isolate the incident channel from a possible return of the reflected signal from the cavity. This isolation is 32 dB at 2.41 GHz. Therefore, this experimental set-up allows us to measure incident and reflected signals that are not affected by external contributions. Finally, the Keysight MSO9254A oscilloscope with a bandwidth of 4 GHz and a sampling frequency of 20 GSa/s makes it possible to measure our signals with a vertical resolution of 1 mV and a horizontal resolution of 1 ps.

The modulator accepts on its channel I a signal with a maximum peak amplitude of 0.32 V. It constrains the exponential growth of the incident signal amplitude (characterised by the envelope generated by the AWG) to stop once this value is reached. In addition with the oscilloscope resolution that constrains the initial amplitude of the incident signal, this also limits the duration of the excitation, which is about a hundred nanoseconds according to the numerically constructed signal, seen Fig. 5. Characterisation of the different elements of the microwave circuit (consisting, as shown in Fig. 6, of an isolator, a circulator, coaxial cables, ...) has been conducted, in term of losses and time delay. Therefore, we recover the amplitudes of the incident and reflected signals at the coaxial connector of the cavity access. Temporal synchronisation was achieved by generating a CW signal at the real part of the zero over 400 ns, and for the cavity replaced by a short circuit. The signal measured on the reflected channel is then the 180° out of phase image of the signal measured on the incident channel, and delayed by 2.4 ns, more or less two periods ($\pm$0.83 ns). Taking into account these effects, the incident and reflected signals at the cavity access can be plotted and compared in term of amplitude and time delay. Thanks to the temporal resolution of the oscilloscope, we can also verify the phase correspondence of the signals.

B. Practical results

Fig. 7 illustrates the result of our measurements with the experimental set-up, for the excitation of a zero of the S-matrix of our cavity. In a similar way to the figure constructed numerically earlier, we observe a reflected signal that is almost zero during the excitation, whereas the incident signal sees its amplitude increasing over time. It therefore brings more and more energy to the cavity. We show here the feasibility of the excitation of a zero of the S-matrix for a microwave device and then the realisation of virtual critical coupling.

The incident signal used for this experimental demonstration has a complex frequency $f_{exci} = 2.4090 - j0.0090$ GHz. Recall that for our $e^{j\omega t}$ convention, this complex frequency with negative imaginary part corresponds to an exponentially growing amplitude. The real part has been slightly tuned to clearly identify the time $t_{r=0}$ for an harmonic excitation. For real frequencies different from even 1 MHz, the reflection was no longer exactly zero at this time (see supplementary materials sec. III). However, we found an imaginary part of the complex excitation frequency similar to the one previously extracted, thus validating our extraction time domain method.

We show the envelope generated by the AWG, duplicated for negative amplitudes in Fig. 7. The amplitude of this envelope takes into account the correction related to the attenuations undergone if it propagated to the cavity access. The cut-off of the excitation is represented by the vertical dotted line. It serves as a reference for identifying the signal reflected during the excitation (in yellow) and the one measured once the excitation is cut off (in red). Thus, we can see that for the time during which the incident signal can be shaped according to the zero, the measured reflected signal has an amplitude in the measurement noise. This can be viewed as the absence of scattering sought by the virtual critical coupling. As soon as the incident signal returns to zero, the energy stored in the cavity is released. The associated signal measured on the oscilloscope follows an exponentially decaying amplitude. It is characterised by a time constant identical to that calculated by

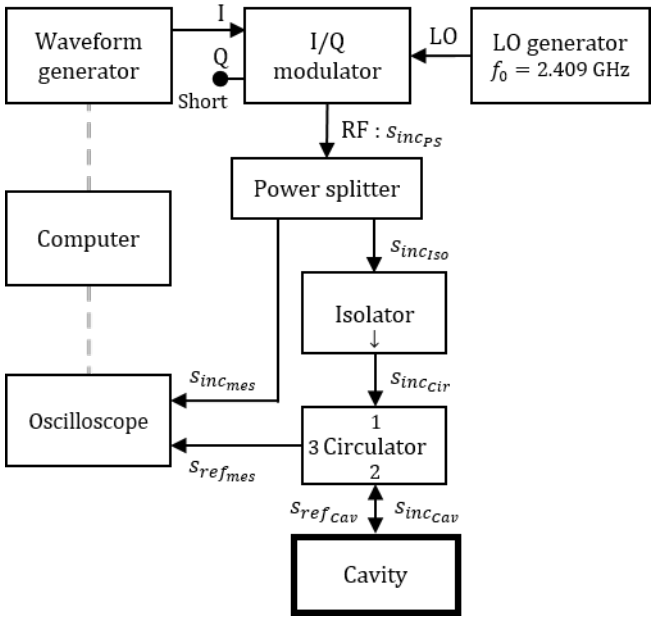

(a)

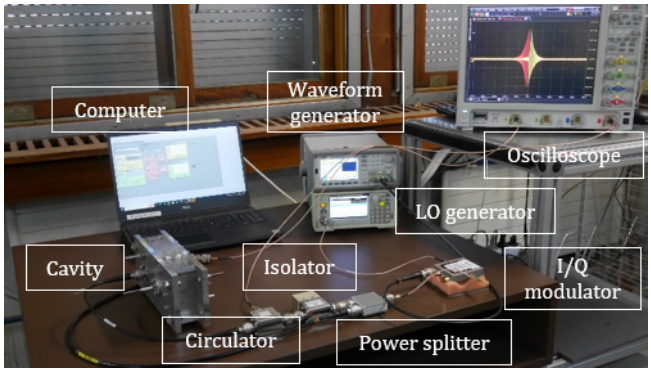

(b)

FIG. 6: (a) Scheme and (b) photograph of the experimental set-up.

the numerical reconstruction. The decay therefore seems to take place for the pole associated with this resonance mode.

VI. CONCLUSION

The experimental implementation of virtual critical coupling to a microwave resonant cavity has been demonstrated. To achieve this, we proposed a time domain method for extracting the scattering system parameters. This relies on the S-matrix measurement and the analysis of the cavity harmonic response over time. It allows the calculation of the singular complex angular frequencies that are the poles and zeros of the S-matrix, taking into account the effect related to the losses in the cavity. The cavity used was not specifically designed for the needs of this experiment. It is therefore possible to replicate our approach for other types of single-access overcoupled cavities of arbitrary shape, in a frequency band in which the

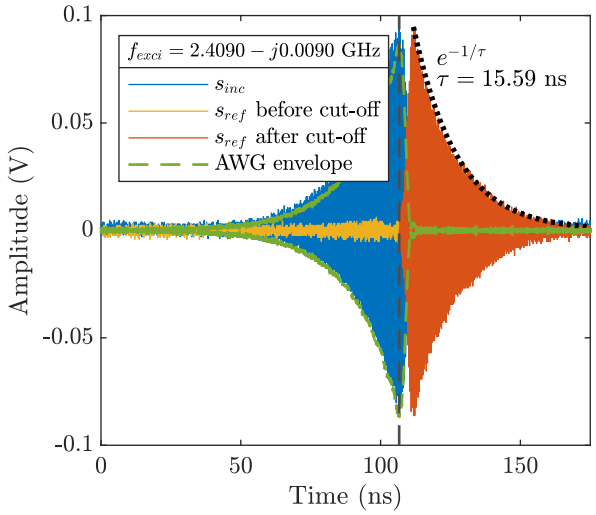

FIG. 7: Observation of a zero of the S-matrix of our cavity through our practical set-up.

resonance modes are isolated.

Moreover, the experimental demonstration of the excitation of an overcoupled cavity without reflection can lead us to consider the principle of a new efficient strategy of plasma ignition in cavity and maybe to a transient time control of the cavity behaviour during plasma ignition process. This strategy would no longer be based on a modification of the system[2,4], but rather on a temporal modulation of the energy generator. This principle reinforces the need to overcome the lossless hypothesis for the realisation of virtual absorption. The cavity will indeed see its load changing during the ignition process, and through it, the intrinsic losses of the cavity and the coupling regime. In addition to the implementation of this matching strategy, the temporality of the excitation and the power level to be reached for the plasma breakdown seem to be major additional challenges to be met, notably from a hardware point of view. A detailed and comparative energy analysis of the different coupling options (critical coupling, virtual critical coupling), among others in the presence of intrinsic losses, may help to better define the limits. This study for the ignition of plasmas in resonant cavities should be the object of our future work.

SUPPLEMENTARY MATERIALS

See (supplementary materials link) for a detailed study of the scattered signal at the excitation cut-off. We also show the measurements made for CW excitation using our experimental set-up. We complete our experimental results on the zero excitation by a comparison with excitations at complex frequencies close to the zero.

AUTHORS DECLARATIONS

The authors have no conflicts to disclose.

ACKNOWLEDGMENTS

The authors would like to thank Béatrice Fragge for her contribution concerning the cavity used in this paper.

DATA AVAILABILITY STATEMENT

The data that support the findings of this study are available from the corresponding author upon reasonable request.

REFERENCES

[1]Y. P. Raizer, *Gas Discharge Physics* (Springer-Verlag Berlin Heidelberg, 1991).
[2]H. Conrads and M. Schmidt, "Plasma generation and plasma sources," Plasma Sources Science and Technology **9**, 441–454 (2000).
[3]A. Lacoste, F. M. Dias, C. Boisse-Laporte, and P. Leprince, "Experimental study of energy coupling and plasma breakdown in a pulsed high frequency resonant cavity," Journal of Applied Physics **89**, 3108–3114 (2001).
[4]F. Silva, K. Hassouni, X. Bonnin, and A. Gicquel, "Microwave engineering of plasma-assisted CVD reactors for diamond deposition," Journal of Physics: Condensed Matter **21**, 364202 (2009).
[5]G. Lerosey, J. de Rosny, A. Tourin, A. Derode, G. Montaldo, and M. Fink, "Time reversal of electromagnetic waves," Phys. Rev. Lett. **92**, 193904 (2004).
[6]V. Mazières, R. Pascaud, L. Liard, S. Dap, R. Clergereaux, and O. Pascal, "Plasma generation using time reversal of microwaves," Applied Physics Letters **115**, 154101 (2019).
[7]V. Mazières, O. Pascal, R. Pascaud, L. Liard, S. Dap, R. Clergereaux, and J.-P. Boeuf, "Space-time plasma-steering source: Control of microwave plasmas in overmoded cavities," Phys. Rev. Applied **16**, 054038 (2021).
[8]D. Kalluri, *Electromagnetics of Time Varying Complex Media: Frequency and Polarization Transformer, 2nd Edition* (CRC Press, 2010).
[9]A. Krasnok, D. G. Baranov, H. Li, M.-A. Miri, F. Monticone, and A. Alù, "Anomalies in light scattering," Adv. Opt. Photon. **11**, 892–951 (2019).
[10]W. R. Sweeney, C. W. Hsu, and A. D. Stone, "Theory of reflectionless scattering modes," Phys. Rev. A **102**, 063511 (2020).
[11]Y. D. Chong, L. Ge, H. Cao, and A. D. Stone, "Coherent perfect absorbers: Time-reversed lasers," Phys. Rev. Lett. **105**, 053901 (2010).
[12]D. G. Baranov, A. Krasnok, and A. Alù, "Coherent virtual absorption based on complex zero excitation for ideal light capturing," Optica **4**, 1457–1461 (2017).
[13]M. Mirmoosa, G. Ptitcyn, V. Asadchy, and S. Tretyakov, "Time-varying reactive elements for extreme accumulation of electromagnetic energy," Phys. Rev. Applied **11**, 014024 (2019).
[14]D. Sounas, "Virtual perfect absorption through modulation of the radiative decay rate," Phys. Rev. B **101**, 104303 (2020).
[15]S. Longhi, "Coherent virtual absorption for discretized light," Opt. Lett. **43**, 2122–2125 (2018).
[16]Q. Zhong, L. Simonson, T. Kottos, and R. El-Ganainy, "Coherent virtual absorption of light in microring resonators," Phys. Rev. Research **2**, 013362 (2020).
[17]A. Marini, D. Ramaccia, A. Toscano, and F. Bilotti, "Metasurface-bounded open cavities supporting virtual absorption: free-space energy accumulation in lossless systems," Opt. Lett. **45**, 3147–3150 (2020).
[18]A. Farhi, A. Mekawy, A. Alu, and D. Stone, "Excitation of absorbing exceptional points in the time domain," (2022).
[19]G. Trainiti, Y. Ra'di, M. Ruzzene, and A. Alù, "Coherent virtual absorption of elastodynamic waves," Science Advances **5** (2019).
[20]L.-P. Euve, P. Petitjeans, A. Maurel, and V. Pagneux, "Transient total absoprtion for water waves : a two port setup," in *APS Division of Fluid Dynamics Meeting Abstracts*, APS Meeting Abstracts (2021) p. A27.007.
[21]M. Cai, O. Painter, and K. J. Vahala, "Observation of critical coupling in a fiber taper to a silica-microsphere whispering-gallery mode system," Phys. Rev. Lett. **85**, 74–77 (2000).
[22]Y. Ra'di, A. Krasnok, and A. Alù, "Virtual critical coupling," ACS Photonics **7**, 1468–1475 (2020).
[23]V. Grigoriev, A. Tahri, S. Varault, B. Rolly, B. Stout, J. Wenger, and N. Bonod, "Optimization of resonant effects in nanostructures via weierstrass factorization," Phys. Rev. A **88**, 011803 (2013).
[24]M. R. Wall and D. Neuhauser, "Extraction, through filter-diagonalization, of general quantum eigenvalues or classical normal mode frequencies from a small number of residues or a short-time segment of a signal. i. theory and application to a quantum-dynamics model," The Journal of Chemical Physics **102**, 8011–8022 (1995).
[25]V. A. Mandelshtam and H. S. Taylor, "Harmonic inversion of time signals and its applications," The Journal of Chemical Physics **107**, 6756–6769 (1997).
[26]J. Wiersig and J. Main, "Fractal weyl law for chaotic microcavities: Fresnel's laws imply multifractal scattering," Phys. Rev. E **77**, 036205 (2008).
[27]U. Kuhl, R. Höhmann, J. Main, and H.-J. Stöckmann, "Resonance widths in open microwave cavities studied by harmonic inversion," Phys. Rev. Lett. **100**, 254101 (2008).
[28]M. Osman and Y. V. Fyodorov, "Chaotic scattering with localized losses: s-matrix zeros and reflection time difference for systems with broken time-reversal invariance," Phys. Rev. E **102**, 012202 (2020).
[29]L. Chen and S. M. Anlage, "Use of transmission and reflection complex time delays to reveal scattering matrix poles and zeros: Example of the ring graph," Phys. Rev. E **105**, 054210 (2022).
[30]K. Pichler, M. Kühmayer, J. Böhm, A. Brandstötter, P. Ambichl, U. Kuhl, and S. Rotter, "Random anti-lasing through coherent perfect absorption in a disordered medium," Nature **567**, 351–355 (2019).
[31]L. Chen, T. Kottos, and S. M. Anlage, "Perfect absorption in complex scattering systems with or without hidden symmetries," Nature Communications **11**, 5826 (2020).
[32]M. F. Imani, D. R. Smith, and P. del Hougne, "Perfect absorption in a disordered medium with programmable meta-atom inclusions," Advanced Functional Materials **30**, 2005310 (2020).
[33]B. W. Frazier, T. M. Antonsen, S. M. Anlage, and E. Ott, "Wavefront shaping with a tunable metasurface: Creating cold spots and coherent perfect absorption at arbitrary frequencies," Phys. Rev. Research **2**, 043422 (2020).
[34]P. del Hougne, K. B. Yeo, P. Besnier, and M. Davy, "On-demand coherent perfect absorption in complex scattering systems: Time delay divergence and enhanced sensitivity to perturbations," Laser & Photonics Reviews **15**, 2000471 (2021).
[35]P. del Hougne, K. B. Yeo, P. Besnier, and M. Davy, "Coherent wave control in complex media with arbitrary wavefronts," Phys. Rev. Lett. **126**, 193903 (2021).
[36]J. Sol, D. R. Smith, and P. del Hougne, "Meta-programmable analog differentiator," Nature Communications **13**, 1713 (2022).
[37]C. Wang, W. R. Sweeney, A. D. Stone, and L. Yang, "Coherent perfect absorption at an exceptional point," Science **373**, 1261–1265 (2021).
[38]S. Suwunnarat, Y. Tang, M. Reisner, F. Mortessagne, U. Kuhl, and T. Kottos, "Non-linear coherent perfect absorption in the proximity of exceptional points," Communications Physics **5**, 2399–3650 (2022).
[39]L. Chen, S. M. Anlage, and Y. V. Fyodorov, "Generalization of wigner time delay to subunitary scattering systems," Phys. Rev. E **103**, L050203 (2021).
[40]B. Fragge, J. Sokoloff, O. Rouzaud, O. Pascal, and M. Orain, "A versatile set-up to study plasma/microwave sources for liquid fuel ignition," Eur. Phys. J. Appl. Phys. **92**, 30903 (2020).
[41]H. A. Haus, *Waves and fields in optoelectronics* (Englewood Cliffs, NJ: Prentice-Hall, 1984).
[42]W. Suh, Z. Wang, and S. Fan, "Temporal coupled-mode theory and the presence of non-orthogonal modes in lossless multimode cavities," IEEE Journal of Quantum Electronics **40**, 1511–1518 (2004).
[43]D. Pozar, *Microwave Engineering, 4th Edition* (Wiley, 2011).